ON-LINE ELECTRON BEAM MEASUREMENTS FOR THE LOS ALAMOS FREE-ELECTRON LASER*

A. H. Lumpkin, R. B. Feldman, D. W. Feldman, and W. E. Stein

Los Alamos National Laboratory
P. O. Box 1663
Los Alamos, NM 87545 USA

Abstract: Recent developments in the electron beam diagnostics used on the Los Alamos Free-Electron Laser (FEL) have extended our on-line, quantitative analysis capability to extraction efficiency and micropulse temporal duration. The FEL's 20-MeV electron beam is 100 μs in length and consists of ~2000 micropulses of 20-ps duration and 46-ns separation. This extreme range of time scales is addressed by employing a combination of synchronized beam deflectors, an electron spectrometer, intensified video cameras, real-time video digitizers, and microcomputers. The tapered wiggler result for extraction efficiency (2%) and results for pulse duration measurements (10-15 ps) by two techniques are presented.

Introduction

An important aspect of understanding the dynamics of the Los Alamos Free-Electron Laser (FEL) is the ability to perform time-resolved diagnostics with the appropriate time resolutions. Our FEL is a mid-infrared (~10μ) oscillator driven by a radio frequency (*rf*) linear accelerator which produces a relativistic 20-MeV electron beam. The relevant time structures are established by the 100-μs-long macropulse which consists of ~2000 micropulses of 20-ps duration separated by 46 ns. The need for an on-line capability for optimizing the laser performance was identified during the oscillator experiments that were reported previously. [1-4] In the case of extraction efficiency, increased optical powers in the resonant cavity can damage optical components and make it difficult to quantify transient cavity losses. So the on-line capability has been implemented via the measurement of the electron beam's energy spectra as a function of time under lasing and nonlasing conditions. [5] This is one of the most important FEL performance parameters. Electron beam peak current as indicated by accelerated charge and micropulse temporal profile is a parameter that has been determined to be critical for improving FEL performance. This latter parameter is characterized on the 10-20 ps time scale by two methods: a combination of *rf* deflector and gated, intensified camera or a streak camera and temporal analyzer. [6]

Experimental Procedures

Diagnostics to determine the energy and temporal distributions of the accelerated, 20-MeV electron beam were located downstream from the wiggler at the end of the beamline. Figure 1 shows a portion of the beamline with the 60° achromatic bend, the wiggler, the *rf* and dipole deflectors, the electron spectrometer, and the diagnostic cameras.

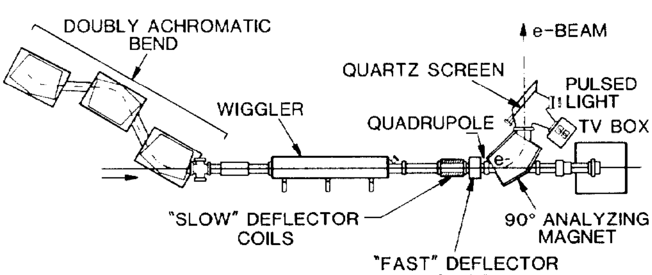

Fig. 1. A portion of the beamline showing the 60° bend, the wiggler, the external deflectors, the quadrupole magnet, and the electron spectrometer.

*Work performed under the auspices of the U.S. Dept. of Energy and supported by the Dept. of Defense U.S. Army Strategic Defense Command.

An energy distribution is obtained by a dispersion of the electrons in a 90° magnetic spectrometer. This energy distribution is analyzed on the macropulse time scale with 10 μs resolution by using the slow dipole deflector that provides 2-cm deflection (orthogonal to the energy axis) in 100 μs at the focal plane. [4] A fused silica screen in the focal plane converts the electron beam energy-time distribution into a visible image via the Cherenkov mechanism. Figure 2 shows an example of such images as recorded by the intensified video camera.

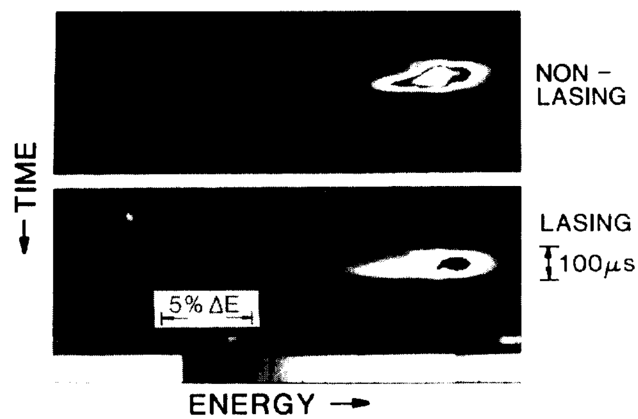

Fig. 2. Sample images from the electron spectrometer focal plane for nonlasing and lasing conditions with 100 μs time coverage.

For the micropulse measurements, the *rf* deflector can be employed with a gated, intensified camera viewing the spectrometer focal plane or, in this case, a screen in the straight-through portion of the beamline (the 90° magnet is turned off) as illustrated in Fig. 3. In this manner a direct measurement of the micropulse durations is obtained. The shorter the micropulse, the shorter the deflection observed. Alternatively, the *rf* deflector is turned off and a Cherenkov screen is viewed by the Hamamatsu C1587 Streak Camera as shown in Fig. 4. The fused silica is at ~45° to the beam direction and the Cherenkov cone is viewed at $\theta = \cos^{-1} 1/\beta n \simeq 46°$ (where $\beta = v/c$ and n = index of refraction) through the special viewing port. The streak camera itself has a limiting resolution of about 2 ps as verified with a mode-locked laser, but the broadband Cherenkov light and the arrival-time effects limit the resolution to ~8-10 ps if no precautions are taken.

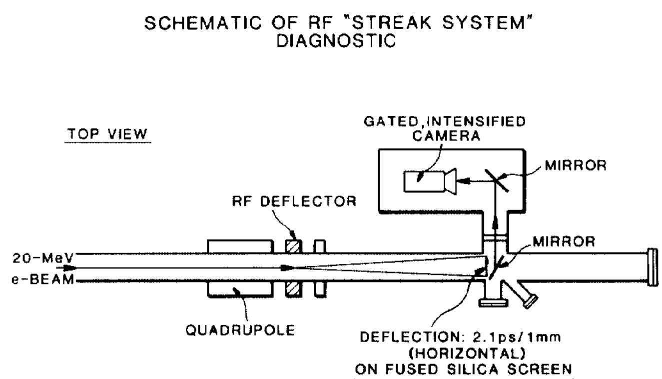

Fig. 3. Schematic of an *rf* "Streak System" diagnostic showing the *rf* deflector, Cherenkov converter screen, and intensified camera.

CH2387-9/87/0000-0212 $1.00 © 1987 IEEE
PAC 1987

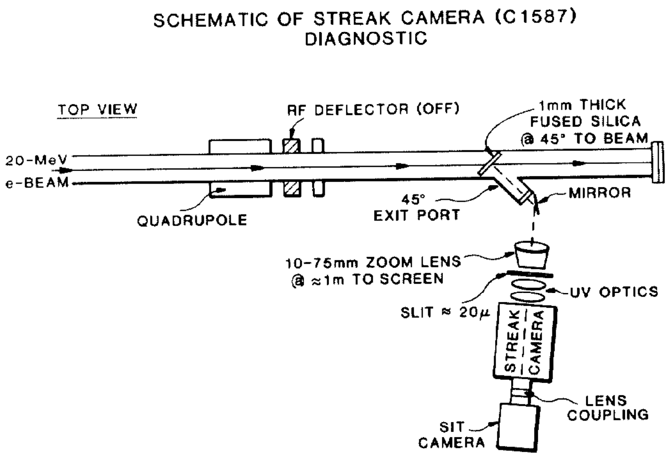

Fig. 4. Schematic of Streak Camera Diagnostic. A second Cherenkov screen is inserted at 45° to the beam direction and viewed through a port at ~45° to the beam direction (close to the Cherenkov angle).

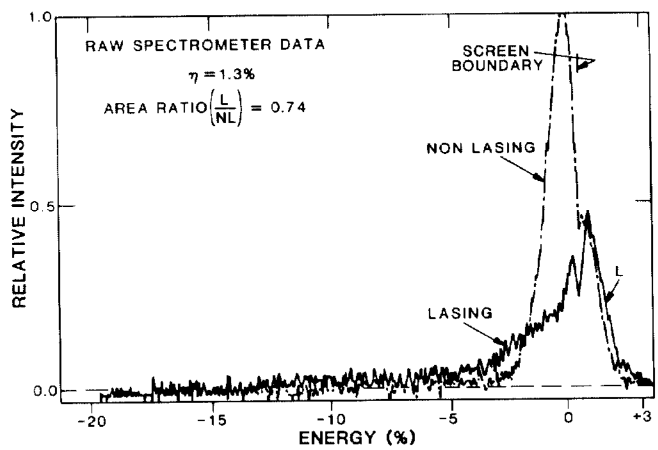

Fig. 5. Raw data plots for the nonlasing-lasing (NL-L) example.

Analysis and Results

Extraction Efficiency

Extraction efficiency is computed from the change in the average energy (centroid) between the nonlasing and lasing conditions. Digital line data from the image in Fig. 2 are shown in Fig. 5. The processing of such data has involved only the subtraction of the camera dark-current reference for both files. Figure 6 shows the flow chart for the analysis program FELGRAF (by R. B. Feldman) in which conversions or corrections for the spectrometer energy calibration, the video camera transfer curve, and the focal plane screen efficiency are applied. The data can also be smoothed by a sliding average routine. Figure 7 shows the results of applying such a program to the data of Fig. 5. It is noted that ratioing the area under the two data files provides a test of the analysis. In the final data, the areas are within 3% while initially the areas differed by 26%. This change is mostly due to the camera transfer curve and the relative insensitivity to the low intensity, lower energy data in the lasing distribution. The final extraction efficiency of 2% is the highest observed in an FEL operating below the microwave region.

Micropulse Duration

Micropulse temporal profiles have been determined in two ways as discussed previously. [6] These results include magnetic bunching effects in the nonisochronous 60° bend.

In the first case, the rf deflector is employed to provide deflections of the 20-MeV beam that correspond to ~2.1 ps/mm

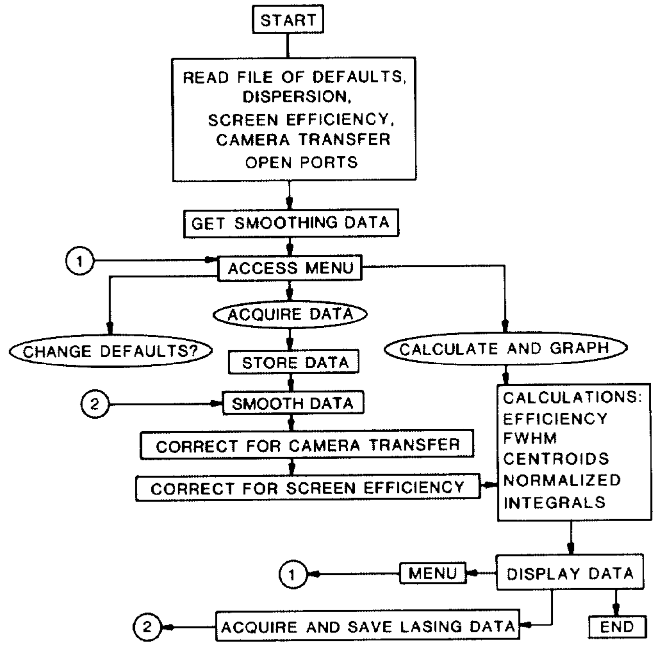

Fig. 6. Flow chart for the extraction efficiency analysis for Fig. 5 with graphic output.

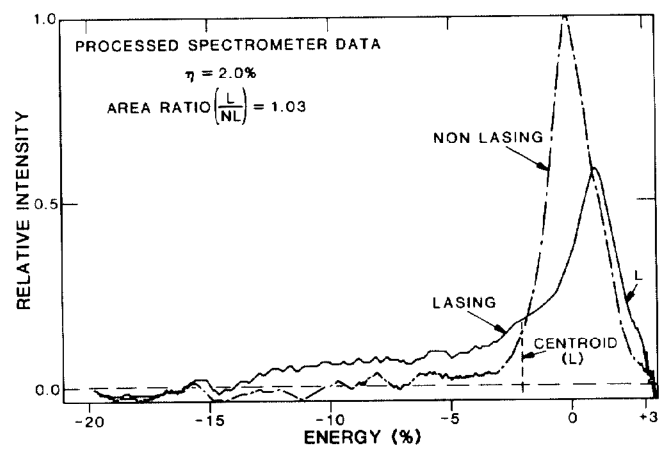

Fig. 7. Processed data plots of the electron spectra for the example in Fig. 5. All corrections have been applied, the data statistically smoothed, and the extraction efficiency determined.

(see Fig. 3). The analysis program for extraction efficiency was basically transformed to calculate time profiles (program FELDELT, by R. B. Feldman). The nondeflected beam spot size and the rf field determined a limiting resolution (Δt_{sys}) of ~7 ps in the case shown in Fig. 8. The total pulse width (Δt_{obs}) is observed as 15 ps and the actual electron beam pulse-width (Δt_p) is estimated as 13 ps by assuming gaussian behavior so that

$$\Delta t_p = \left[(\Delta t_{obs})^2 - (\Delta t_{sys})^2\right]^{1/2} . \qquad (1)$$

A peak current greater than 200A is indicated. It should be noted that at lower accelerated charge we did observe shorter pulses.

In the second method using a Hamamatsu streak camera (see Fig. 4) and Hamamatsu temporal analyzer, additional results are obtained. In the top of Fig. 9, the initial streak image is shown. Deflection plates in the streak tube have converted the vertical direction into a time axis. An analysis window is set on the image and the average time profile computed and displayed. In the lower portion of the figure, the time profile was rotated for

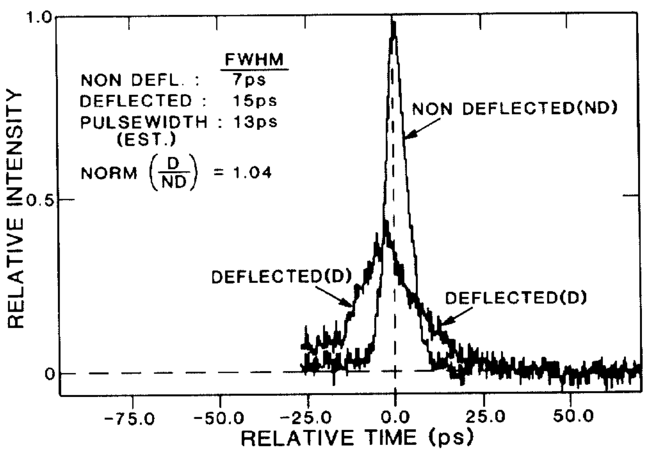

Fig. 8. Time profiles with the *rf* deflector off (nondeflected) and on (deflected). These data show the system limiting resolution of about 7 ps and the total observed pulse width of ~15 ps. These data indicate a micropulse of about 13 ps duration.

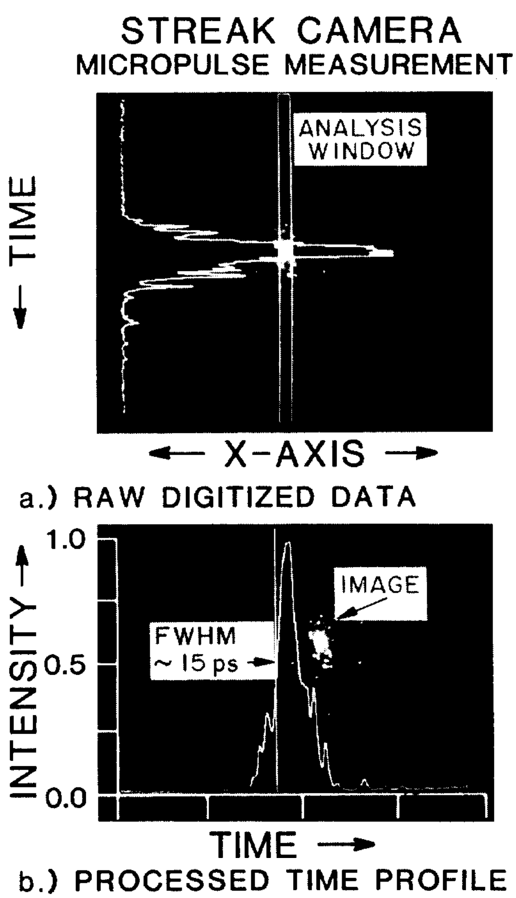

Fig. 9. Sample data from the Hamamatsu C1587 streak camera and processed by the C2280 temporal analyzer. The figure shows: a) raw digitized data and its time profile and b) the processed time profile redisplayed on the horizontal axis showing a FWHM of 15 ps.

display onto the horizontal axis, the data smoothed, and the full width at half maximum (FWHM) calculated. This total observed width corresponded to 15 ps. This includes the system electronic resolution limit of 4 ps and the as yet unquantified effects of dispersion and arrival time. An estimated total resolution limit of 8 ps would be reasonable. Again this information is available in an on-line manner. Both techniques are being evaluated and qualified as part of the program to provide micropulse optimization.

Summary and Conclusion

In summary, we have demonstrated that these techniques can be employed with great advantage in an on-line manner to the study of the Los Alamos FEL. For both extraction efficiency and micropulse temporal duration, we can provide both tune-up or optimization capability and quantitative analysis. These techniques have proven invaluable in our attaining higher extraction efficiencies.

References

[1] Brian E. Newnam, et al., "Optical Performance of the Los Alamos Free-Electron Laser," IEEE Journal of Quantum Electronics, Vol. QE-21, No. 7, pp. 867-881, July 1985.

[2] Richard L. Sheffield, et al., "Electron-Beam Diagnostics and Results for the Los Alamos Free-Electron Laser," IEEE Journal of Quantum Electronics, Vol. QE-21, No. 7, pp. 895-903, July 1985.

[3] Roger W. Warren, Brian E. Newnam, and John C. Goldstein, "Raman Spectra and the Los Alamos Free-Electron Laser," IEEE Journal of Quantum Electronics, Vol. QE-21, No. 7, pp. 882-888, July 1985.

[4] A. H. Lumpkin, et al., "Time-resolved Electron Beam Diagnostics for the Los Alamos Free-Electron Laser Oscillator Experiment," IEEE Trans. Nucl. Sci., Vol. NS-30, p. 3139, August 1983.

[5] A. H. Lumpkin and R. B. Feldman "On-line Extraction Efficiency Analyses for the Los Alamos Free-Electron Laser," Eighth International Free-Electron Laser Conference, September 1-5, 1986, Glasgow, Scotland, LA-UR-86-2983.

[6] A. H. Lumpkin and D. W. Feldman, "Diagnostics of the Los Alamos Free-Electron Laser Using Streak Systems," Eighth International Free-Electron Laser Conference, September 1-5, 1986, Glasgow, Scotland, LA-UR-86-2984.